The final publication is available at

https://doi.org/10.1016/j.marpolbul.2022.113487

Additional Information

1   *Ex vivo* **exposure to titanium dioxide and silver nanoparticles mildly affect sperm of**

2   **gilthead seabream (*Sparus aurata*) - a multiparameter spermiotoxicity approach**

3

4

5   **Reprotoxicity; gametes; marine fish; short-term exposure; sub-lethal effects;**

6   **quiescent sperm**

7

8   Carvalhais A[1], Oliveira IB[2*], Oliveira H[1,], Oliveira CCV[3], Ferrão L[3,4], Cabrita E[3], Asturiano,

9   JF[4], Guilherme S[1], Pacheco M[1], Mieiro CL[1]

10

11   [1]CESAM and Department of Biology, University of Aveiro, Campus Universitário de

12   Santiago, 3810-193 Aveiro, Portugal

13   [2]Interdisciplinary Centre of Marine and Environmental Research (CIIMAR), University of

14   Porto, 4450-208 Matosinhos, Portugal

15   [3]Centre of Marine Sciences (CCMAR), University of Algarve, Campus de Gambelas,

16   8005-139 Faro, Portugal

17   [4]Grupo de Acuicultura y Biodiversidad, Instituto de Ciencia y Tecnología Animal,

18   Universitat Politècnica de València, Spain

19

20   [*]Corresponding author

21

22

23   **Highlights**

24   • TiO$_2$ NP and Ag NP induced low effects on *Sparus aurata* sperm quality

25   • Ag NP decreased sperm total motility at supra environmental levels

26   • TiO$_2$ NP induced depletion of all the antioxidant response

27   • Ag NP induced SOD depletion at the lowest and intermediate concentrations

28

29 **Abstract (max 150 words)**

30 Nanoparticles (NP) are potentially reprotoxic, which may compromise the success of

31 populations. However, the reprotoxicity of NP is still scarcely addressed in marine fish.

32 Therefore, we evaluated the impacts of environmentally relevant and supra

33 environmental concentrations of titanium dioxide (TiO_2: 10 to 10000 µg.L^{-1}) and silver

34 NP (Ag: 0.25 to 250 µg.L^{-1}) on the sperm of gilthead seabream (*Sparus aurata*). We

35 performed short-term direct exposures (*ex vivo*) and evaluated sperm motility, head

36 morphometry, mitochondrial function, antioxidant responses and DNA integrity. No

37 alteration in sperm motility (except for supra environmental Ag NP concentration),

38 head morphometry, mitochondrial function, and DNA integrity occurred. However,

39 depletion of all antioxidants occurred after exposure to TiO_2 NP, whereas SOD

40 decreased after exposure to Ag NP (lowest and intermediate concentration).

41 Considering our results, the decrease in antioxidants did not indicate vulnerability

42 towards oxidative stress. TiO_2 NP and Ag NP induced low spermiotoxicity, without

43 proven relevant ecological impacts.

44

1. Introduction

The unique physicochemical properties of nanoparticles (NP) are attractive to industry, medicine and consumer products, leading to their massive production and widespread dispersal into the environment, namely into the marine ecosystems as the ultimate destination of contaminants (Kurwadkar et al., 2015; Shaalan et al., 2016). Titanium dioxide NP (TiO_2 NP) and silver NP (Ag NP) are used in a broad range of products, including sunscreens, cosmetics, dyes, antimicrobial products, whose production corresponds to 89 – 97% of the total NP emissions into the environment. These NP are considered the most relevant concerning human and environmental hazards (Keller et al., 2013).

The available information on the toxicity of NP points towards oxidative stress, cyto- and genotoxicity, changes in immunological alterations and histopathological lesions (Auguste et al., 2019; Barmo et al., 2013; Canesi et al., 2010; Magesky & Pelletier, 2018; Mieiro et al., 2019; Vignardi et al., 2015). However, limited data exist regarding their toxic potential in reproduction (reprotoxicity). The available studies on male nanoreprotoxicity mainly focused on mammals suggest that NP induce testicular toxicity through hormonal imbalance and oxidative stress, which negatively affects sperm DNA integrity, the total number of sperm count, and motility related parameters (de Brito et al., 2020; Ogunsuyi et al., 2020; Olugbodi et al., 2020; Santonastaso et al., 2019). These harmful effects in mammalian sperm functionality were related to NP' ability to cross blood-testis-barrier (De Jong et al., 2008; Falchi et al., 2016; Lan & Yang, 2012). However, several studies reported low physiological permeability of mammalian sperm plasma membrane to exogenous substances, as well as no intracellular uptake of NP by endocytosis due to the rigidity of sperm

69 membrane (Barkalina et al., 2014; Falchi et al., 2016; Taylor et al., 2014, 2015). Still,

70 toxicity occurs through direct contact of NP by binding to the sperm plasma membrane

71 surface without intracellular uptake (Barkalina et al., 2014; Taylor et al., 2014, 2015).

72 NP may act as surface acting agents inducing indirect toxic effects mainly due to

73 adsorption instead of internal uptake (Handy et al., 2011).

74 Despite no information on the uptake process is found for fish sperm, their plasma

75 membrane differs from others by presenting a high content in cholesterol and

76 polyunsaturated lipid species, which controls the quality of sperm and varies among

77 species (Beirão et al., 2012a; Engel et al., 2020; Labbé & Loir, 1991). This lipidic

78 composition of the membrane increases permeability, promotes enzyme activity and

79 intercellular membrane fusion, characteristics that allow sperm cells to fulfill their

80 function at fertilization (Beirão et al., 2012a; Wassall & Stillwell, 2009).

81 Fish sperm are in a quiescent metabolic condition in the testes, characterized by an

82 immotile state. After spawning, in fish with external fertilization, sperm faces abrupt

83 alterations in the environmental medium (e.g., alteration of osmolality and exposure

84 to increasing oxygen), which trigger sperm activation. The osmotic pressure, namely,

85 hyperosmotic shock, is the main factor controlling the activation of sperm motility in

86 marine teleosts (Zilli et al., 2008). During activation, spermatozoa undergo functional

87 modifications such as increasing membrane fluidity and motility (Alavi et al., 2019;

88 Islam & Akhter, 2012), making them highly vulnerable. The presence of contaminants

89 in water, such as NP, may potentiate the natural vulnerability of these cells, impairing

90 their fertilization ability and, consequently, reproductive success.

91 Due to the relevance of this issue and the role of sperm in reproduction, along with the

92 ethical advantage resulting from minimally invasive sperm collection techniques in fish,

5

93   sperm quality analysis has been proposed as an indicator for reproductive success with

94   application in environmental risk assessment (Cabrita et al., 2014; Gallo and Tosti.,

95   2020). The most commonly used parameters to assess sperm quality are sperm count,

96   motility pattern, viability, morphology, mitochondrial function (Erraud et al., 2017) and

97   DNA integrity analysis (*e.g.*, through the comet assay) (Shamsi et al., 2011).

98   Additionally, the antioxidant profile is also being used as a specific and suitable

99   biomarker, as it can provide information on sperm vulnerability to reactive oxygen

100   species (ROS) (Hook et al., 2014).

101   Accordingly, the main objective of this study was to evaluate the effects of

102   environmentally relevant concentrations of TiO_2 NP and Ag NP on the sperm of

103   gilthead seabream (*Sparus aurata*) upon a short-term direct exposure (*ex vivo*).

104   Gilthead seabream is a predator and euryhaline teleost. It is one of the most important

105   fish species in the Mediterranean aquaculture (Nielsen et al., 2021) and a model

106   organism in research, specifically in environmental risk assessment and

107   cryopreservation protocols (Beirão et al., 2012a,b; Marques et al., 2019). It is a

108   protrandric sequential hermaphrodite species in which the reproductive season takes

109   several months. One of the main advantages of using seabream is the direct and easy

110   sampling of sperm, simply by placing a syringe outside the urogenital pore (Beirão et

111   al., 2019). Their spermatozoa display typical aquasperm morphology: long tail,

112   spherical head without an acrosome, and a short or absent midpiece, as described in

113   other fishes of the Sparidae family (Beirão et al., 2012b; Marco-Jiménez et al., 2008).

114   To achieve a thorough assessment of sperm quality after exposure to NP, this study

115   adopted a multiparameter approach by evaluating sperm motility, morphometry,

116   mitochondrial function, antioxidant responses and DNA integrity.

117 Understanding the spermiotoxic effects of NP' contributes to recognizing their

118 ecological impacts. Predicting these impacts can contribute to the establishment of

119 effective prevention measures, avoiding later recovery costs at population and

120 community levels.

121

122 **2. Materials and Methods**

123 **2.1. Preparation and characterization of nanoparticle suspensions and silver nitrate**

124 **solution**

125 **2.1.1. Titanium dioxide nanoparticles**

126 TiO_2 NP, namely Aeroxide®P25 (purity ≥ 99.5% CAS# 13463-67-7), were provided by

127 Sigma-Aldrich. Crystalline phase and crystallite size were identified by the X-ray

128 diffraction technique XRD, using a Philips X'Pert X-ray diffractometer equipped with a

129 Cu Kα monochromatic radiation source ($\lambda \alpha K = 1.4060$ nm). A stock suspension (1

130 mg.mL^{-1}) was prepared in distilled water (dH$_2$O) by sonication with an ultrasonic

131 processor (Sonics Vibra-Cell), for 15 minutes (min) at 100W, with 5:1 pulses on/off. The

132 dispersion was performed in an ice bath. TiO_2 NP working suspensions (10, 100, 1000

133 and 10000 μg.L^{-1}) were prepared with non-activated medium, namely saline solution

134 (NaCl; 9 g.L^{-1}). The TiO_2 NP structure was confirmed by scanning transmission electron

135 microscopy (STEM), using a JEOL 2200FS, JEOL Ltd., Japan model. TiO_2 NP size

136 distribution in 0.9 % NaCl was determined by Dynamic Light Scattering (DLS) analysis,

137 using a ZetasizerNano ZSP (Malvern Instruments Ltd.) at 25 °C. Measurements were

138 done in triplicate with over 13 sub-runs in fresh suspensions and also 1 h after

139 preparation to mimic the *ex vivo* (direct exposure) conditions.

140

2.1.2. Silver nanoparticles and silver nitrate

141

142 Ag NP dispersion [10 nm particle size (TEM - Transmission Electron Microscopy),

143 0.02 mg.mL^{-1} in aqueous buffer, containing sodium citrate as stabilizer] was supplied

144 by Sigma-Aldrich. Ag NP structure was confirmed by STEM, using a JEOL 2200FS, JEOL

145 Ltd., Japan model. DLS analysis was performed to determine Ag NP behavior in 0.9 %

146 NaCl, as previously described for TiO$_2$ NP.

147 Ag NP stock suspension (0.0025 mg.mL^{-1}) was prepared in dH2O and Ag NP working

148 suspensions (0.25, 25 and 250 µg.L^{-1}) were prepared in 0.9 % NaCl. Stock and working

149 suspensions were vortexed before the next dilution.

150 To allow the discrimination of the involvement of dissolved Ag form on the measured

151 responses, Ag$^+$ solutions were also prepared (see section 2.3.). AgNO$_3$ (purity ≥ 99%,

152 ACS reagent, CAS# 7761-88-8) was provided by Sigma-Aldrich. AgNO$_3$ stock solution

153 (0.0040 mg.mL^{-1}, [Ag$^+$] = 0.0025 mg.mL^{-1}) was prepared in dH$_2$O and AgNO$_3$ working

154 solutions (0.40, 40, 400 µg.L^{-1}, [Ag$^+$] = 0.25, 25 and 250 µg.L^{-1}) were prepared in 0.9 %

155 NaCl by successive dilutions of the stock suspension, as previously performed for Ag

156 NP. Stock and working suspensions were vortexed before proceeding with the next

157 dilution. We will refer to the use of Ag$^+$ present in AgNO$_3$ as Ag$^+$.

158

2.2. Semen collection

159

160 Sperm was collected from sexually mature gilthead seabream (*Sparus aurata*) reared

161 males (2 years old, approximately 0.5 kg), provided by Aqualvor Lda fish farm (Lagos,

162 Portugal) during their reproductive season (December–February in the South of

163 Portugal). Sperm was released by abdominal massage and retrieved with a 1 mL

164 syringe, without the needle. Samples were kept in microtubes inside polystyrene

165   support to avoid direct contact with ice (~ 4 °C), until analysis. All samples showing

166   urine contamination were rejected. A total of 12 sperm samples corresponding to

167   different males were used.

168

169   **2.3. Experimental design**

170   Semen was directly exposed (*ex vivo*) to several concentrations of TiO_2 NP or Ag NP, in

171   two independent trials. TiO_2 NP tested concentrations reflected the levels found at

172   Mediterranean marine waters (water column and top surface layer) (Labille et al.,

173   2020), as well as supra-environmental concentrations. Ag NP levels replicated the

174   levels found in French wastewater (influent and effluent) (Deycard et al., 2017) and

175   supra-environmental concentrations. Four concentrations of TiO_2 NP (10, 100, 1000

176   and 10000 $\mu g.L^{-1}$) and three concentrations of Ag NP (0.25, 25 and 250 $\mu g.L^{-1}$) were

177   tested. Since Ag NP can undergo oxidative dissolution in water (Zhang et al., 2016), the

178   same concentrations of Ag^+ (0.25, 25 and 250 $\mu g.L^{-1}$) were also assessed to evaluate

179   the contribution of the dissolved Ag form. The *ex vivo* exposures (1:10, v/v semen and

180   exposure medium [0.9 % NaCl and NP], respectively to achieve a final sperm

181   concentration of ~$2x10^7$ cells/ml) lasted 1 h with gentle agitation performed every 15

182   min. The exposure was performed at 4° C to avoid sperm degradation (Gallego and

183   Asturiano, 2019).

184   After exposure, sperm was directly collected for motility (section 2.4) and

185   morphometry (section 2.5) evaluation. For the remaining analysis, samples were

186   centrifuged in a refrigerated centrifuge (Eppendorf 5415R) at 800 g for 15 min at 4° C,

187   and the supernatant was discarded to remove NP and seminal plasma. Then, the pellet

188 was resuspended in 0.9 % NaCl to achieve a final concentration of 2×10^7 cells.mL^{-1} and

189 divided into several aliquots for further evaluation.

190

191 **2.4. Sperm motility**

192 Motility was assessed using the CASA system (ISAS - Integrated System for Sperm

193 Analysis; Proiser, Valencia, Spain) coupled to a phase-contrast microscope (Nikon E-

194 200; Nikon, Tokyo, Japan) with an ISAS camera (Gallego and Asturiano, 2018, 2019).

195 For sperm activation, 5 µL of artificial seawater (1100 mOsm.kg^{-1}) were added to 1 µL

196 of the cell suspension and motility was recorded at 15, 30, 45, and 60 s post-activation

197 in the same field. Samples exposed to each NP and concentration (n=12 males) were

198 analyzed four times per treatment. Image sequences were captured with a 10x

199 negative phase contrast objective, saved and analyzed afterwards using the ISAS

200 software. The software settings were adjusted to gilthead seabream sperm using 25

201 frames per second and considering the head area of 1 to 90 µm^2. Spermatozoon was

202 considered motile when VCL (curvilinear velocity) was higher than 10 µm.s^{-1}. CASA

203 rendered the percentage of motile cells in the sperm sample. The assessed parameters

204 were: the total motility (TM, %), expressed as the percentage of motile cells, and the

205 curvilinear velocity (VCL, mm/s), which corresponds to the average velocity of a

206 spermatozoon head along its curvilinear trajectory (Gallego et al. 2014).

207

208 **2.5. Sperm morphometry**

209 Seabream sperm were analyzed for morphometric changes using the protocol

210 developed by Marco-Jiménez et al. (2008). Briefly, after exposure to NP, 4 µL of sperm

211 were fixed in a 1:50 ratio (v:v) in 2.5% glutaraldehyde solution prepared in PBS. An

212 aliquot of the previous dilution was then placed in a slide and visualized using a 100

213 x·negative phase contrast objective, using immersion oil (Nikon Plan Fluor) in an

214 Eclipse E400 Nikon microscope connected to an ISAS camera. Images were acquired

215 and the morphometric parameters were analyzed using the computer-assisted sperm

216 analysis (ASMA - Automated Sperm Morphometry Analysis) software (Sperm Class

217 Analyser, Morfo Version 1.1, Valencia, Spain). The morphometric parameters

218 determined in the sperm head were: head length (μm), width (μm), perimeter (μm),

219 and area (μm^2). A total of 200 sperm cells were analyzed per male (n= 10) and

220 treatment.

221

222 **2.6. Sperm DNA integrity**

223 An aliquot of each sample was diluted in 0.9 % NaCl to a final concentration of 1×10^4

224 cells.mL^{-1}. Comet assay was performed according to Collins (2004), adapted with a

225 system of eight gels per slide as described by Guilherme et al. (2014) and adapted for

226 gilthead seabream sperm according to Cabrita et al. (2005). Briefly, the slides were

227 immersed in a lysis solution (2.5 M NaCl, 100 mM EDTA, 10 mM Tris, 1% Triton X-100,

228 and 1% lauryl sarcosine, pH 10) at 4 °C for 1 h. Dithiothreitol (10 mM) was added to the

229 lysis solution and gels were immersed for 30 min at 4 °C. Subsequently, lithium

230 diiodosalicylate (4 mM), was added to the solution and gels were immersed for 90 min

231 at 4 °C.

232 Slides were then placed horizontally in the electrophoresis tank with electrophoresis

233 solution (0.3 M NaOH, 1 mM Na2–EDTA, pH 12) for 20 min at 4 °C. Electrophoresis was

234 conducted at a fixed voltage of 20 V, a current of 300 mA for 10 min at 4 °C.

235 Afterwards, slides were drained and immersed in a neutralizing solution (0.4 M Tris, pH

236 7.5) for 5 min at 4 °C. This procedure was performed twice and slides were then placed

237 in a solution of 70% ethanol for 2 min, 90% ethanol for 2 min and followed by pure

238 ethanol for 2 min. Lastly, slides were left to dry in the air and stored for later analysis.

239 Positive control was also prepared in 0.9 % NaCl and previously incubated with a

240 damage promoter [hydrogen peroxide (H_2O_2) 50 mM] for 15 min at 4 °C (Azqueta et

241 al., 2011).

242 For comet visualization, slides were stained with ethidium bromide (20 $\mu g.mL^{-1}$). Fifty

243 nucleoids were observed per gel, using a Leica DM2000 LED fluorescence microscope

244 (x400 magnification). DNA damage was quantified by visual scoring of nucleoids,

245 according to Collins (2004). Nucleoids were scored into five classes according to the tail

246 length and intensity, from 0 (no tail) to 4 (almost all DNA in tail indicating highly

247 damaged DNA). The genetic damage indicator (GDI) was calculated according to the

248 formula:

249
$$\text{GDI} = \sum \% \text{ nucleoids class } i \times i$$
250
251 where i is the number of each defined class (ranging within 0 - 4) and GDI values were

252 inherently expressed as arbitrary units on a scale of 0 - 400 per 100 scored nucleoids.

253

254 **2.7. Sperm mitochondrial function and antioxidant activity**

255 Mitochondrial function was evaluated as described by Oliveira et al. (2009) with some

256 modifications for gilthead seabream. Briefly, we evaluated mitochondrial function by

257 using Rhodamine 123/propidium iodide (Rh123/PI) dual fluorescent staining. Rh123 is

258 a cationic fluorescent dye (1 $mg.mL^{-1}$ in methanol [-20 °C]) was diluted in dH_2O to a

259 concentration of 0.1 $mg.mL^{-1}$ and 10 μL were added to 400 μL of each cell suspension

260 (1 to 2 x 10^7 cells.mL^{-1}). Samples were incubated at 4 °C for 30 min, in the dark,

261 allowing Rh123 to accumulate in functional active mitochondria. Afterwards, samples

262 were centrifuged for 10 min at 500 g, the supernatant was discarded and the pellet

263 was resuspended in NaCl. Then, 10 µL of PI (0.1 mg.mL^{-1}), used to mark unviable cells,

264 were added to the sample 5 min before flow cytometric analyses (Attune® Acoustic

265 Focusing Cytometer, ThermoFisher Scientific). The instrument was equipped with a

266 blue laser (488 nm) for excitation. Green fluorescence from Rh123 was detected in BL1

267 sensor, through a 530/30 filter, while the red fluorescence of PI was collected through

268 a 574/26 filter. Sperm cells were gated based on the forward (FS) vs. side scatter (SC)

269 properties. At least 10, 000 events were acquired for each sample. The percentage of

270 sperm with functional mitochondria was calculated as the ratio of cells positive for

271 Rh123 (PI+Rh123+/PI-Rh123+) *vs.* total cell number.

272 For the biochemical analysis, spermatozoa were lysed to release antioxidants. First,

273 sperm samples were centrifuged at 4° C for 10 min at 10000 g, and the supernant was

274 discarded. Then, the pellet was resuspended with PBS 0.1% Triton X-100, vortexed and

275 frozen in liquid nitrogen. Afterwards, samples were thawed at room temperature,

276 centrifuged at 5000 g for 5 min at 4 °C, and the supernatant removed. Lastly, samples

277 were diluted with 0.01 M PBS and subsequently frozen in liquid nitrogen and stored at

278 -80 °C until analyses.

279 Catalase (CAT) activity analysis was based on those described by Claiborne (1985) and

280 Giri et al. (1996). Briefly, the assay mixture consisted of 10 µL phosphate buffer (0.05

281 M, pH 7.0), 195 µL hydrogen peroxide (10 mM) and 10 µL of the sample. The

282 absorbance was monitored for 3 min at intervals of 10 s at 25 °C. The CAT activity was

283 analyzed at 240 nm and expressed in µmol H_2O_2 consumed.min^{-1}.mg $protein^{-1}$ (Ɛ =

284   43.5 M^{-1} cm^{-1}).

285   Glutathione peroxidase (GPx) activity was assayed according to the method described

286   by Mohandas et al. (1984), modified by Athar & Iqbal (1998). The assay mixture

287   consisted of 90 µL phosphate buffer (0.05 M, pH 7.0), X ml EDTA (10 mM), 30 µL

288   sodium azide (10 mM), 30 µL glutathione reductase (GR; 2.4 U/ml), 30 µL reduced

289   glutathione (GSH; 10 mM), 30 µL NADPH (1.5 mM), 30 µL H_2O_2 (2.5 mM) and 30 µL of

290   the sample. The absorbance was read at 340 nm each 30 s for a 5 min period at 25 °C

291   and expressed in nmol NADPH oxidized.min^{-1}.mg $protein^{-1}$ ($\varepsilon = 6.22 \times 10^3$ M^{-1} cm^{-1}).

292   Superoxide dismutase (SOD) activity was determined through the spectrophotometric

293   enzymatic kit (RANSOD TM, Randox), adapted to a microplate. Xanthine and xanthine

294   oxidase were used to produce superoxide radicals that react with 2-(4-iodophenyl)-3-

295   (4-nitrophenol)-5-phenyltetrazolium chloride (INT) originating a red dye of formazan.

296   The assay consisted in adding 10 µL of diluted PMS, 210 µL of Mixed substrate (R1) and

297   30 µL of xanthine oxidase (R2) .The absorbance was read at 550 nm during 3:30 min at

298   25 °C. SOD activity was expressed in U.mg $protein^{-1}$, where a unit of SOD induced the

299   inhibition of 50% of the INT reduction rate.

300   The total protein content was determined in the PMS according to Bradford (1976),

301   adapted to a microplate, using bovine serum albumin as a standard. Absorbance

302   reading was performed at 595 nm.

303   All antioxidants and proteins were measured using a microplate reader (Synergy™ H1

304   BioTeck®).

305

306   **2.8. Statistical analyses**

307   The effect of the different treatments (independent variables) on the different

308 dependent variables (motility, morphometry, GDI, DNA damage classes, enzymatic

309 antioxidants, and mitochondrial function) was analyzed using one-way ANOVA,

310 followed by a multiple comparisons test. Graphical validation tools were used to verify

311 ANOVA assumptions. Whenever assumptions were not fulfilled, data were evaluated

312 with the equivalent non-parametric test. To satisfy the assumptions of ANOVA,

313 percentage data (*viz*., sperm motility and mitochondrial function) were arcsine-

314 transformed. A paired-samples t-test, and the equivalent non-parametric (Mann-

315 Whitney U test), was conducted to distinguish the effects of Ag NP from those of Ag^+.

316 The results were expressed as mean and standard deviation. The statistical analyses

317 were performed using IBM.SPSS®, version 27.0.1, and all the statistical tests were

318 considered significant when $p < 0.05$. All the descriptive data have been collated into

319 supplementary tables.

320

321 **3. Results**

322 **3.1. Characterization of the nanoparticle suspensions**

323 **3.1.1. Titanium dioxide nanoparticles**

324 The standard spheroid irregular shape of TiO_2 NP (Aeroxide© P25) with a primary size

325 of a mean particle diameter of 19.34 ± 6.72 nm in the stock suspension was confirmed

326 by STEM (Fig. S1). The histograms of the different sizes of TiO_2 NP showed a unimodal

327 right-skewed distribution, with approximately 60% of the values ranging from 10 to 20

328 nm in the stock suspension, as well as in all TiO_2 NP working suspensions. The XRD

329 analysis demonstrated the presence of the crystalline phase anatase (86.8%) and rutile

330 (13.2%). DLS analysis of TiO_2 NP stock suspension (1 mg.mL^{-1}) in dH_2O showed the

331 presence of agglomerates with an average size of NP of 189.0 ± 80.2 nm. The mean

332   hydrodynamic diameters of TiO_2 NP agglomerates in the tested suspensions (in NaCl)

333   were 235.32 ± 17.35, 239.84 ± 63.98, 252.46 ± 51.76 and 690.95 ± 121.59 nm at 10,

334   100, 1000 and 10000 $\mu g.L^{-1}$, respectively.

335

336   **3.1.2. Silver nanoparticles**

337   STEM analysis showed that silver dispersion (stock suspension) had a spherical

338   appearance with a mean primary size particle diameter of 21.50 ± 8.27 nm (Fig. S2).

339   The histogram of the frequency distribution of different sizes of Ag NP showed a

340   unimodal right-skewed distribution, with nearly 35, 55, and 80% of the values ranging

341   from 10 to 20 nm in the stock suspension and Ag NP working suspensions of 250 $\mu g.L^{-1}$

342   and 25 $\mu g.L^{-1}$, respectively. For the 0.25 $\mu g.L^{-1}$ working suspension of Ag NP, 87.50% of

343   the values ranged from 4 to 10 nm. DLS analysis of Ag NP stock suspension (0.0025

344    $mg.mL^{-1}$) in dH_2O revealed the presence of agglomerates with an average size of

345   142.73 ± 13.74 nm. The mean size of the agglomerates in the tested suspensions (in

346   NaCl) was 130.52 ± 7.89, 134.29 ± 42.28 and 230.04 ± 32.57 nm for 0.25, 25, and 250

347    $\mu g.L^{-1}$, respectively.

348

349   **3.2. Sperm motility and morphometry**

350   The CASA system analysis, carried out at different time points (15, 30, 45, and 60 s

351   post-activation), showed that increasing concentrations of TiO_2 NP did not affect

352   sperm TM, as no significant differences were observed among groups (Table S1; Fig.

353   1A). Similar to TM, VCL also did not show significant differences (Table S1; Fig. 2A).

354   Concerning Ag NP exposure, TM decreased in the highest concentration in comparison

355   with the control group, for all the different time points post-activation (Table S2). TM

356　remained unaltered after the exposure of sperm to Ag^+ in all the recorded post-

357　activation times (Table S2; Fig. 1B). TM was similar between the corresponding

358　exposure levels Ag NP and Ag^+ (Table S3). VCL decreased in the highest Ag NP

359　concentration concerning to the intermediate concentration, at 15 s post-activation

360　($H_{(3,40)}$ = 8.629, $p \leq 0.05$), while in the other post-activation times, VCL remained

361　unaltered. After the exposure to Ag^+, VCL also remained unaltered in all recorded post-

362　activation times (Table S2). For the concentration 25 $\mu g.L^{-1}$ at 30 s post-activation

363　($U_{(1,16)}$ = 11.000, $p \leq 0.05$) and 250 $\mu g.L^{-1}$ at 45 s post-activation ($U_{1,16)}$ = 11.500, $p \leq$

364　0.05) the VCL was lower for Ag^+ than for Ag NP (Fig. 2B).

365　The morphometric analysis showed no significant differences for any of the studied

366　parameters after exposure to all NP tested, TiO_2 and both Ag NP and Ag^+ (Tables S1

367　and S2; Fig. 3). The absence of differences between Ag NP and Ag^+ was also observed

368　for all the morphometric parameters (Table S3).

369

370　**3.3. DNA integrity in sperm**

371　After TiO_2 NP exposure, gilthead seabream sperm did not show significant alterations

372　in the GDI among treatments (Table S1; Fig. 4A). To better understand the distribution

373　of DNA damage throughout the range of the tested concentrations, GDI classes were

374　analyzed individually. Again, no statistically significant differences were observed

375　between treatments in all classes (Table S1). Similarly to TiO_2 NP, no significant

376　alterations in the GDI values among treatments were found for Ag NP or Ag^+ (Table S2;

377　Fig. 4B) as well as for DNA damage classes (Table S2). No significant differences were

378　found between each concentration of Ag NP and Ag^+ for GDI (Table S3), nor for all

379　assessed DNA damage classes (Table S3).

3.4. Sperm mitochondrial function and antioxidant activity

No significant differences were detected between the mitochondrial function of sperm exposed to TiO_2 NP and the control treatment, as well as among the tested TiO_2 NP concentrations (Table S1; Fig. 5A). The same result was observed for Ag NP and Ag^+ (Table S2; Fig. 5B). The paired samples, between each concentration of Ag NP and Ag^+, presented no significant differences (Table S3).

The studied antioxidants (CAT, GPx and SOD) showed decreased activities in all TiO_2 NP treatments in comparison with control ($H_{(4,46)} = 17.381$, $p = 0.002$; $H_{(4,45)} = 17.721$, $p \leq 0.001$; $H_{(4,46)} = 18.654$, $p \leq 0.001$ for CAT, GPx, and SOD respectively) (Table S1; Fig. 6A, C, E). CAT and GPx activities remained unaltered after the exposure of sperm to Ag NP (Fig. 6B, D), though the activity of SOD decreased significantly in the two lowest Ag NP concentrations relatively to control ($H_{(3,36)} = 8.401$; $p \leq 0.05$) (Table S2; Fig. 6F).

When sperm cells were exposed to Ag^+, CAT activity decreased significantly in both the lowest and the highest concentrations relatively to control ($H_{(3,40)} = 16.518$; $p \leq 0.001$) (Table S2; Fig. 6B), while a significant decrease was observed in the GPx activity of sperm exposed to the lowest concentration of Ag^+ ($H_{(3,36)} = 14.700$; $p \leq 0.01$) (Table S2; Fig. 6D). SOD activity decreased significantly in the lowest and intermediate Ag^+ concentrations in relation to control ($H_{(3,40)} = 17.530$; $p \leq 0.001$) (Table S2; Fig. 6F).

The paired-sample t-test showed that CAT activity was lower in the highest Ag^+ concentration ($U_{(1,20)} = 20.000$; $p \leq 0.05$) (Table S3; Fig. 6B). In the case of SOD, lower activity was also found for both the lowest and the highest concentrations of Ag^+ ($U_{(1,18)} = 15.000$; $p \leq 0.05$; $U_{(1,20)} = 20.000$; $p \leq 0.05$ for 0.25 and 250 µg.L^{-1}, respectively) (Table S3; Fig. 6F). No differences were found between Ag NP and Ag^+ for GPx activity (Table S3; Fig. 6D).

4. Discussion

The importance of addressing sperm quality for environmental risk assessment was just recently acknowledged. Sperm quality is intrinsically related to the fertilization ability being crucial for species maintenance and propagation. Thus, understanding contaminant effects and mode of action in sperm allows reliably predicting the environmental risk posed by these substances and setting recommendations regarding their presence in the environment. Notwithstanding the suitability of sperm quality, namely motility, as an indicator of reproductive success with application in environmental risk assessment, a limited number of studies exist focusing on the impact of contaminants on sperm function (Gallego and Asturiano, 2018, 2019; Gallo et al., 2020), particularly those related to the effects of NP in aquatic organisms. Despite that, the existing information points towards the impairment of sperm function after exposure to NP (Gallo et al., 2016; Han et al., 2019; Kowalska-Góralska et al., 2019; Özgür et al., 2018a,b,c, 2019, 2020).

4.1. Sperm motility and morphometry

The majority of the physiological processes of fish sperm is determined by motility as fertilization relies on sperm encounters with the oocyte (Cosson, 2019). For that reason, this is the most studied functional parameter in sperm.

The effects of iron oxide NP (Fe_3O_4 NP), zinc oxide NP (ZnO NP), silica oxide NP (SiO NP), and copper oxide NP (CuO NP) in freshwater and marine fish sperm showed a general reduction of motility after *ex vivo* short-term exposures (Kowalska-Góralska et al., 2019; Özgür et al., 2018b, 2018c, 2019). The same occurred after TiO_2 NP *ex vivo* exposures in marine organisms (fish - *Capoeta trutta* and bivalve -*Tegillarca granosa*).

428 These studies showed a general decrease in different motility parameters (VCL,

429 straight-line velocity – VSL, and angular path velocity – VAP) after 2 h of direct

430 exposure to TiO_2 NP (10 to 10000 µg.L-1 of TiO_2 NP) (Han et al., 2019; Özgür et al.,

431 2020).). On the contrary, our results revealed no alteration of the motility parameters

432 (TM and VCL) following TiO_2 NP exposure, despite the adoption of the same exposure

433 procedure (direct exposure) and the same range of TiO_2 NP concentrations (10 to

434 10000 µg.L-1 of TiO_2 NP). In the case of the rainbow trout (*Oncorhynchus mykiss*),

435 Özgür et al. (2018a) also reported no alteration in VCL after 3 h of direct exposure to

436 TiO_2 NP concentrations ranging from 10 to 50000 µg.L^{-1}. However, these authors found

437 contradictory results for the remaining parameters (VAP, VSL and percentage of

438 linearity). The discrepancies between studies may be due to the duration of exposure,

439 different sensitivity among the assessed parameters, and species-specificities. Distinct

440 species-specific mechanisms were already reported, pointing towards a higher

441 inherent vulnerability of freshwater sperm due to their physiological maladaptation to

442 hypoosmotic shock (Billard & Cosson, 1990). Moreover, marine fish have a higher

443 polyunsaturated/unsaturated fatty acids ratio than freshwater fish (Drokin, 1993),

444 which confers higher fluidity to marine fish sperm membranes and thus higher

445 resistance.

446 To the best of our knowledge, no studies assessed the effects of Ag NP in the motility

447 of marine organisms' sperm. The available data focused on humans (short-term direct

448 exposure) and other mammals (long-term *in vivo* exposure), reporting a general

449 decrease in sperm motility (TM, VCL, VSL, and VAP) (Moretti et al., 2013; Olugbodi et

450 al., 2020; Shehata et al., 2021; Wang et al., 2017). Similarly, in the present study, TM

451 also decreased, but only at the highest Ag NP concentration (250 µg.L^{-1}). The sperm

452   motility of gilthead seabream might be regulated by ROS-mediated processes (Zilli et

453   al., 2017). The decrease in motility after exposure to the highest Ag NP concentration

454   is not accompanied by DNA damage, impairment of the mitochondrial function nor

455   alteration in the antioxidants (see section 4.3). Thus, we anticipate that Ag NP might

456   affect motility by a physical interaction with the sperm surface. We hypothesize two

457   different mechanisms: impairment of the motility by mechanical processes or by

458   interactions of the Lewis-acid of the NP surface with Lewis-acid thiol groups of the

459   membrane (Taylor et al., 2014). Mechanical processes induced by the large

460   agglomerates attached to the flagellum may delay motility, whereas NP interaction

461   with the membrane structure/composition may interfere with membrane

462   transporters. Taylor et al. (2014) suggested that gold NP affected the motility of bull

463   sperm by interacting with the membrane.

464   The higher toxicity of the Ag ion was previously described for zebrafish gills (*Danio*

465   *rerio*) (exposure via water for 48 h) (Griffitt et al., 2009) and the marine diatom

466   (*Chaetoceros curvisetus*) (Lodeiro et al., 2017). However, the higher toxicity of the Ag

467   ion compared to Ag NP was not possible to confirm since no alterations of the motility

468   were found for Ag^+.

469   Like motility, sperm morphometry is a reliable indicator of sperm quality (Gallego et

470   al., 2014; Marco-Jiménez et al., 2008). Any alterations in its shape may interfere with

471   the swimming capacity or the penetration of the sperm head through the oocyte

472   micropyle. Our results showed that the analyzed head morphometric parameters were

473   unaltered after TiO_2 NP, Ag NP and Ag^+ exposure. No studies were found regarding

474   using this tool to describe the effects of NP in sperm. Nevertheless, a single study with

475   goldfish (*Carassius auratus*) showed no effects on sperm head length, width and area

476   after an instant exposure (5 s) to mercury (1 to 100000 µg.L^{-1}). However, the levels of

477   those parameters increased after 24 h exposure (Van Look & Kime, 2003), suggesting

478   that morphometric changes are time-dependent and that instant exposures are not

479   likely to induce alterations. We forecasted the absence of alterations in sperm

480   morphometry was related to no or slight motility effects induced by TiO$_2$ NP and Ag NP

481   exposure, respectively. Plus, sperm was exposed in its quiescent stage (see section

482   4.4), as gilthead seabream sperm motility only lasts a few minutes.

483   Exposing non-motile sperm, though not fully mimicking the post-release moment, is

484   the trade-off to going deeper into the effects of water contaminants on these cells.

485   We, therefore, predict that these *ex vivo* assays reflect the impacts of NP at the post-

486   release moment without underestimating the risk to spermatozoa and its ecological

487   consequences.

488

489   **4.2. Sperm DNA integrity**

490   Assessing DNA damage at individual levels allows predicting any changes at the

491   population level. The loss of DNA integrity was previously reported in the sperm of

492   humans and aquatic organisms following direct exposure to NP (Gallo et al., 2016,

493   2018; Han et al., 2019; Santonastaso et al., 2019, 2020; Wang et al., 2017). DNA

494   damage was reported even at low TiO$_2$ NP concentrations in human sperm (1, 10 µg.L-

495   1) and in a marine bivalve (10 and 100 µg.L-1) (Santonastaso et al., 2019; Han et al.,

496   2019). Unlike these studies, no DNA damage occurred for the seabream sperm

497   suggesting less vulnerability to this NP. The lower vulnerability of seabream sperm

498   compared with the marine bivalve may be because the sperm of bivalves are active

499   when exposed to NP, as they are motile for more than 24 h. Sessile organisms exhibit

500 extensive periods of sperm motility than fish, as their spermatozoa must travel longer

501 distances to find the egg to fertilize (Gallego et al., 2014). The same can be considered

502 for human sperm since assays use ejaculated sperm and, therefore, motile cells.

503 In the case of Ag NP, there are no comparable studies on aquatic organisms. However,

504 a decrease in DNA integrity occurred after direct exposure (1 h) of human sperm to

505 high concentrations of Ag NP (200000 µg.L^{-1} and 400000 µg.L^{-1}) (Wang et al., 2017).

506 Contrary to human sperm, no DNA damage occurred in our study with sperm of

507 gilthead seabream after exposure to Ag NP (0.25 to 250 µg.L^{-1}) and Ag$^+$ ion (0.25 to 250

508 µg.L^{-1}). Yet, the disparity of concentrations between studies does not allow further

509 comparisons.

510

511 **4.3. Sperm mitochondrial function and antioxidant activity**

512 ROS formation is the predominant molecular mechanism of NP toxicity to sperm,

513 which induces impairment of the mitochondrial function and changes in membrane

514 composition (Gallo et al., 2016, 2018; Özgür et al., 2018b, 2020; Ogunsuyi et al., 2020).

515 The vulnerability towards ROS is related to the sperm plasma membrane high content

516 of cholesterol and polyunsaturated fatty acids (Costantini et al., 2010). Plus, the small

517 volume of cytoplasm and thus the low levels of antioxidants depicted by sperm

518 contribute to their susceptibility to ROS and oxidative stress (Słowińska et al., 2013).

519 In this work, SOD activity decreased after exposure to low and intermediate

520 concentrations of Ag NP, and an overall depletion of the antioxidant activity (CAT, GPx,

521 and SOD) occurred after exposure to TiO$_2$ NP. As antioxidants are the first line of

522 defense against ROS (Costantini et al., 2010; Słowińska et al., 2013), their depletion

523 might suggest that gilthead seabream spermatozoa are vulnerable to ROS production.

The excess of ROS might inhibit the enzymes of oxidative phosphorylation and glycolysis, limiting the production of ATP (De Lamirande et al., 1997) and subsequently impairing mitochondrial function. Therefore, concomitantly to the depletion of the activity of antioxidants, it was expected to find impairment of the mitochondrial function of sperm exposed to the NP. Yet, no alteration of the mitochondrial function emerged after exposure to NP. The absence of mitochondrial impairment may be due to the quiescent stage of spermatozoa during the *ex vivo* exposures. In quiescent spermatozoa, mitochondria are at a basal metabolic rate encompassing low energy mobilization, low oxygen consumption (Alavi et al., 2019), and inhibition of some enzymes that regulate the respiratory chain (Christen et al., 1987). Plus, in quiescent spermatozoa, no interference of the ROS-mediated signal cascade, that triggers activation, occurred. Hence, the depletion of the antioxidants suggests two possible mechanisms of action by the NP: enzyme inhibition by NP, more severe in the case of TiO_2 NP, or by the promotion of a favourable antioxidant condition. Indeed, both TiO_2 NP and Ag NP can have antioxidant properties, a characteristic that depends on the extracts used in their synthesis (Keshari et al., 2020; Bedlovičová et al., 2021; Rajeswari et al., 2021). For Ag NP these mechanisms are concentration-dependent, as it does not occur at the highest concentration.

Previous studies reported increasing lipid peroxidation either in fish spermatozoa directly exposed to TiO_2 NP or in the testis of rats after long-term oral exposure to Ag NP (Özgür et al., 2020; Shehata et al., 2021). Assessment of lipid damage would have been convenient in our samples but was not possible due to methodological limitations.

548   **4.4. Inference for the sperm-shield effects**

549   The direct exposure of NP on fish sperm occurs in semen (seminal plasma and

550   spermatozoa) and utilizes quiescent sperm. Seminal plasma protects spermatozoa

551   from oxidative damage and thus may have functioned as a shield against NP oxidative

552   potential (Kowalski & Cejko, 2019).

553   Another identified inference is related to the NP characteristics such as charge, size,

554   coating, and concentration. NP-specific features affect their ability to induce toxicity

555   and access the cells (Cameron et al., 2018). Lankoff et al. (2012) found that the

556   agglomeration state affects NP's cellular localization and toxicity. These authors found

557   that the smaller the agglomerates size, the greater its toxicity, pointing to higher

558   toxicity of Ag NP than TiO2 NP. However, the small agglomerate size for Ag NP (235 -

559   691 nm *vs*. 131 -230 nm, for TiO2 NP and Ag NP, respectively) did not reflect higher

560   toxicity, as most of the effects occurred after TiO2 NP exposure.

561   The lower Ag NP toxicity may also be related to the sodium citrate coating. This coating

562   stabilizes the NP and limits its ability to agglomerate. It also reduces the dissolution of

563   Ag NP into Ag ion, which is generally considered more toxic (Fahmy et al., 2019).

564

565   **5. Conclusions**

566   Our study reports the effects of TiO$_2$ NP and Ag NP on *Sparus aurata* sperm through a

567   multiparameter approach. The results showed no alteration in sperm TM (except for

568   the supra environmental concentration of Ag NP), VCL, morphometry, mitochondrial

569   function, and DNA integrity. However, TiO$_2$ NP induced a decrease in all the

570   antioxidants for all concentrations and Ag NP induced SOD depletion at the lowest and

571   intermediate concentrations. Nevertheless, this antioxidant depletion had no impact

572 on the sperm performance. Although the *ex vivo* exposure of *S. aurata* sperm to NP

573 was performed with quiescent cells, this is a suitable approach to simulate the sperm

574 post-release process. Our findings indicate a low vulnerability of *S. aurata* sperm to

575 these NP, translated into absence or low risk after release to the marine environment,

576 with no evidence of relevant ecological impacts. Nevertheless, further studies are

577 required to identify *in vivo* long-term effects of these NP on the reproductive

578 processes of marine species and their mechanism of action.

579

591

592 **References**

593 Alavi, S. M. H., Cosson, J., Bondarenko, O., & Linhart, O. (2019). *Theriogenology* Sperm

594   motility in fishes: (III) diversity of regulatory signals from membrane to the

595   axoneme. *Theriogenology*, *136*, 143–165.

596   https://doi.org/10.1016/j.theriogenology.2019.06.038

597   Athar, M., & Iqbal, M. (1998). Ferric nitrilotriacetate promotes N-diethylnitrosamine-

598   induced renal tumorigenesis in the rat: implications for the involvement of

599   oxidative stress. *Carcinogenesis*, *19*, 1133–1139.

600   Auguste, M., Lasa, A., Pallavicini, A., Gualdi, S., Vezzulli, L., & Canesi, L. (2019).

601   Exposure to TiO 2 nanoparticles induces shifts in the microbiota composition of

602   *Mytilus galloprovincialis* hemolymph. *Science of the Total Environment*, *670*, 129–

603   137. https://doi.org/10.1016/j.scitotenv.2019.03.133

604   Azqueta, A., Gutzkow, K. B., Brunborg, G., & Collins, A. R. (2011). Towards a more

605   reliable comet assay; optimising agarose concentration, unwinding time and

606   electrophoresis conditions. Mutat. Res. 724, 41–45.

607   10.1016/j.mrgentox.2011.05.010

608   Barkalina, N., Charalambous, C., Jones, C., & Coward, K. (2014). Nanotechnology in

609   reproductive medicine: Emerging applications of nanomaterials. *Nanomedicine:*

610   *Nanotechnology, Biology, and Medicine*, *10*(5), e921–e938.

611   https://doi.org/10.1016/j.nano.2014.01.001

612   Barmo, C., Ciacci, C., Canonico, B., Fabbri, R., Cortese, K., Balbi, T., Marcomini, A.,

613   Pojana, G., Gallo, G., & Canesi, L. (2013). *In vivo* effects of n-TiO 2 on digestive

614   gland and immune function of the marine bivalve *Mytilus galloprovincialis*.

615   *Aquatic Toxicology*, *132–133*, 9–18.

616   https://doi.org/10.1016/j.aquatox.2013.01.014

617   Bedlovičová, Zdenka, Imrich Strapáč, Matej Baláž, and Aneta Salayová. 2020. "A Brief

618   Overview on Antioxidant Activity Determination of Silver Nanoparticles"

619   *Molecules* 25, no. 14: 3191. https://doi.org/10.3390/molecules25143191

620   Beirão, J., Zilli, L., Vilella, S., Cabrita, E., Fernández-Díez, C., Schiavone, R., & Herráez,

621   M. P. (2012a). Fatty acid composition of the head membrane and flagella affects

622   Sparus auratasperm quality. *Journal of Applied Ichthyology*, *28*(6), 1017–1019.

623   http://doi.org/10.1095/biolreprod.108.068296

624   Beirão, J., Zilli, L., Vilella, S., Cabrita, E., Schiavone, R., & Herráez, M. P. (2012b).

625   Improving sperm cryopreservation with antifreeze proteins: Effect on gilthead

626   seabream (*Sparus aurata*) plasma membrane lipids. *Biology of Reproduction*,

627   *86*(2), 1–9. https://doi.org/10.1095/biolreprod.111.093401

628   Billard, R., & Cosson, M. (1990). The energetics of fish motility. In C. Gagnon (Ed.),

629   *Control of Sperm Motility: Biological and Clinical Aspects* (pp. 153–173). CRC

630   Press.

631   Bradford, M. M. (1976). A Rapid and Sensitive Method for the Quantitation Microgram

632   Quantities of Protein Utilizing the Principle of Protein-Dye Binding. *Analytical*

633   *Biochemistry*, *254*, 248–254.

634   Cabrita, E., Martínez-Páramo, S., Gavaia, P. J., Riesco, M. F., Valcarce, D. G.,

635   Sarasquete, C., Herráez, M. P., & Robles, V. (2014). Factors enhancing fish sperm

636   quality and emerging tools for sperm analysis. *Aquaculture*, *432*, 389–401.

637   https://doi.org/10.1016/j.aquaculture.2014.04.034

638   Cabrita, E., Robles, V., Cuñado, S., Wallace, J. C., Sarasquete, C., & Herráez, M. P.

639   (2005). Evaluation of gilthead sea bream*, Sparus aurata,* sperm quality after

640   cryopreservation in 5ml macrotubes. *50*, 273–284.

641   https://doi.org/10.1016/j.cryobiol.2005.02.005

642   Cameron, S. J., Hosseinian, F., & Willmore, W. G. (2018). A current overview of the

643   biological and cellular effects of nanosilver. *International Journal of Molecular*

644   *Sciences*, *19*(7), 1–40. https://doi.org/10.3390/ijms19072030

645   Canesi, L., Fabbri, R., Gallo, G., Vallotto, D., Marcomini, A., & Pojana, G. (2010).

646   Biomarkers in *Mytilus galloprovincialis* exposed to suspensions of selected

647   nanoparticles (Nano carbon black , C60 fullerene , Nano-TiO 2 , Nano-SiO 2).

648   *Aquatic Toxicology*, *100*(2), 168–177.

649   https://doi.org/10.1016/j.aquatox.2010.04.009

650   Chapman, D. (1975). Fluidity and phase transitions of cell membranes. In

651   *Biomembranes* (Vol. 7, pp. 1–9). https://doi.org/10.1007/978-1-4684-7668-2_1

652   Christen, R., Gatti, J. -L, & Billard, R. (1987). Trout sperm motility: The transient

653   movement of trout sperm is related to changes in the concentration of ATP

654   following the activation of the flagellar movement. *European Journal of*

655   *Biochemistry*, *166*(3), 667–671. https://doi.org/10.1111/j.1432-

656   1033.1987.tb13565.x

657   Claiborne, A. (1985). Catalase activity. In: Handbook of methods in oxygen radical

658   research; Greenwald RA (ed); CRC Press: Boca Raton, FL, USA, 1985; pp. 283–284.

659   ⌜⌝SEP⌞⌟

660   Collins, A. R. (2004). The comet assay for DNA damage and repair: Principles,

661   applications, and limitations. *Applied Biochemistry and Biotechnology - Part B*

662   *Molecular Biotechnology*, *26*(3), 249–261. https://doi.org/10.1385/MB:26:3:249

663   Cosson, J. (2019). Fish Sperm Physiology: Structure, Factors Regulating Motility, and

664   Motility Evaluation. In Y. Bozkurt (Ed.), *Biological Research in Aquatic Science,*

665   *IntechOpen* (pp. 1–26).

666   Costantini, D., Rowe, M., Butler, M. W., & McGraw, K. J. (2010). From molecules to

667   living systems: Historical and contemporary issues in oxidative stress and

668   antioxidant ecology. *Functional Ecology*, *24*(5), 950–959.

669   https://doi.org/10.1111/j.1365-2435.2010.01746.x

670   de Brito, J. L. M., Lima, V. N. de, Ansa, D. O., Moya, S. E., Morais, P. C., Azevedo, R. B.

671   de, & Lucci, C. M. (2020). Acute reproductive toxicology after intratesticular

672   injection of silver nanoparticles (AgNPs) in Wistar rats. *Nanotoxicology*, *14*(7),

673   893–907. https://doi.org/10.1080/17435390.2020.1774812

674   Deycard, V. N., Schäfer, J., Petit, J. C. J., Coynel, A., Lanceleur, L., Dutruch, L., et al.

675   (2017). Chemosphere. *Chemosphere*, *167*(C), 501–511.

676   http://doi.org/10.1016/j.chemosphere.2016.09.154

677   De Jong, W. H., Hagens, W. I., Krystek, P., Burger, M. C., Sips, A. J. A. M., & Geertsma,

678   R. E. (2008). Particle size-dependent organ distribution of gold nanoparticles after

679   intravenous administration. *Biomaterials*, *29*(12), 1912–1919.

680   https://doi.org/10.1016/j.biomaterials.2007.12.037

681   De Lamirande, E., Jiang, H., Zini, A., Kodama, H., & Gagnon, C. (1997). Reactive oxygen

682   species and sperm physiology. *Reviews of Reproduction*, *2*(1), 48–54.

683   https://doi.org/10.1530/ror.0.0020048

684   Drokin, S. I. (1993). Phospholipids and fatty acids of phospholipids of sperm from

685   several freshwater and marine species of fish. *Comp. Biochem. Physiol.*, *104B*(2),

686   423–428.

687   Engel, K. M., Dzyuba, V., Ninhaus-silveira, A., Veríssimo-silveira, R., Dannenberger, D.,

688   Schiller, J., Steinbach, C., & Dzyuba, B. (2020). Sperm lipid composition in early

689   diverged fish species: Internal vs. external mode of fertilization. *Biomolecules*,

690   *10*(2), 1–25. https://doi.org/10.3390/biom10020172

691   Erraud, A., Bonnard, M., Duflot, A., & Geffard, A. (2017). Assessment of sperm quality

692   in palaemonid prawns using Comet assay : methodological optimization.

693   *Environmental Science and Pollution Research*, *25*(12), 11226–11237.

694   https://doi.org/10.1007/s11356-017-8754-6

695 Fahmy, H. M., Mosleh, A. M., Elghany, A. A., Shams-Eldin, E., Abu Serea, E. S., Ali, S. A.,

696   & Shalan, A. E. (2019). Coated silver nanoparticles: Synthesis, cytotoxicity, and

697   optical properties. *RSC Advances*, *9*(35), 20118–20136.

698   https://doi.org/10.1039/c9ra02907a

699 Falchi, L., Bogliolo, L., Galleri, G., Ariu, F., Zedda, M. T., Pinna, A., Malfatti, L., Innocenzi,

700   P., & Ledda, S. (2016). Cerium dioxide nanoparticles did not alter the functional

701   and morphologic characteristics of ram sperm during short-term exposure.

702   *Theriogenology*, *85*(7), 1274-1281.e3.

703   https://doi.org/10.1016/j.theriogenology.2015.12.011

704 Gaiser, B. K., Fernandes, T. F., Jepson, M., Lead, J. R., Tyler, C. R., & Stone, V. (2009).

705   Assessing exposure, uptake and toxicity of silver and cerium dioxide nanoparticles

706   from contaminated environments. *Environmental health : a global access science*

707   *source*, *8 Suppl 1*(Suppl 1), S2. https://doi.org/10.1186/1476-069X-8-S1-S2

708 Gallego, V., Pérez, L., Asturiano, J. F., & Yoshida, M. (2014). Sperm motility parameters

709   and spermatozoa morphometric characterization in marine species: A study of

710   swimmer and sessile species. *Theriogenology*, *82*(5), 668–676.

711   https://doi.org/10.1016/j.theriogenology.2014.05.026

712 Gallego, V. & Asturiano, J.F. (2018). Sperm motility in fish: technical applications and

713   perspectives through CASA-Mot systems. *Reproduction, Fertility and Development,*

714   *30*(6), 820-832. https://doi.org/10.1071/RD17460

715 Gallego, V. & Asturiano, J.F. (2019). Fish sperm motility assessment as a tool for

716   aquaculture research, a historical approach. *Reviews in Aquaculture, 11*, 697-724.

717   https://doi.org/10.1111/raq.12253

718 Gallo, A., Boni, R., Buttino, I., & Tosti, E. (2016). Spermiotoxicity of nickel nanoparticles

719   in the marine invertebrate *Ciona intestinalis* (ascidians). *Nanotoxicology*, *10*(8),

720   1096–1104. https://doi.org/10.1080/17435390.2016.1177743

721 Gallo, A., Boni, R., & Tosti, E. (2020). Gamete quality in a miltistressor environment.

722   *Environment International*, *138*, 105627.

723   http://doi.org/10.1016/j.envint.2020.105627

724 Gallo, A., Manfra, L., Boni, R., Rotini, A., Migliore, L., & Tosti, E. (2018). Cytotoxicity and

725   genotoxicity of CuO nanoparticles in sea urchin spermatozoa through oxidative

726   stress. *Environment International*, *118*(May), 325–333.

727   https://doi.org/10.1016/j.envint.2018.05.034

728 Gallo, A., & Tosti, E. (2020). Reproductive Processes of Marine Animals as Biomarker

729   for Environmental Stress Impact, 1–16.

730 Giri, U., Iqbal, M., & Athar, M. (1996). Porphyrine-mediated photosensitization has a

731   weak tumor promoting activity in mouse skin: possible role of in situ generated

732   reactive oxygen species. *Carcinogenesis*, *17*(9), 2023–2028.

733 Griffitt, R. J., Hyndman, K., Denslow, N. D., & Barber, D. S. (2009). Comparison of

734   molecular and histological changes in zebrafish gills exposed to metallic

735   nanoparticles. *Toxicological Sciences*, *107*(2), 404–415.

736   https://doi.org/10.1093/toxsci/kfn256

737 Guilherme, S., Santos, M. A., Gaivão, I., & Pacheco, M. (2014). Genotoxicity Evaluation

738   of the Herbicide Garlon V and Its Active Ingredient (Triclopyr) in Fish (*Anguilla*

739   *anguilla* L.) Using the Comet Assay. *Environmental Toxicology*, *March*, 1073–1081.

740   https://doi.org/10.1002/tox

741 Han, Y., Shi, W., Rong, J., Zha, S., Guan, X., Sun, H., & Liu, G. (2019). Exposure to

742   Waterborne nTiO2 Reduces Fertilization Success and Increases Polyspermy in a

743   Bivalve Mollusc: A Threat to Population Recruitment. *Environmental Science and*

744   *Technology*, *53*(21), 12754–12763. https://doi.org/10.1021/acs.est.9b03675

745 Handy, R. D., Al-Bairuty, G., Al-Jubory, A., Ramsden, C. S., Boyle, D., Shaw, B. J., &

746   Henry, T. B. (2011). Effects of manufactured nanomaterials on fishes: a target

747   organ and body systems physiology approach. *Journal of Fish Biology*, *79*(4), 821–

748   853. http://doi.org/10.1080/10934520701792779

749 Hook, S. E., Gallagher, E. P., & Batley, G. E. (2014). The Role of Biomarkers in the

750   Assessment of Aquatic Ecosystem Health. *Integrated Environmental Assessment*

751   *and Management*, *10*(3), 327–341. https://doi.org/10.1002/ieam.1530

752 Islam, M. S., & Akhter, T. (2012). Tale of Fish Sperm and Factors Affecting Sperm

753   Motility: A Review. *Advances in Life Sciences*, *1*(1), 11–19.

754   https://doi.org/10.5923/j.als.20110101.03

755 Keshari, A. K., Srivastava, R., Singh, P., Yadav, V. B., & Nath, G. (2020). Journal of

756   Ayurveda and Integrative Medicine. *Journal of Ayurveda and Integrative Medicine*,

757   *11*(1), 37–44. http://doi.org/10.1016/j.jaim.2017.11.003

758 Keller, A. A., McFerran, S., Lazareva, A., & Suh, S. (2013). Global life cycle releases of

759   engineered nanomaterials. *Journal of Nanoparticle Research*, *15*(6).

760   https://doi.org/10.1007/s11051-013-1692-4

761 Kowalska-Góralska, M., Dziewulska, K., & Kulasza, M. (2019). Effect of copper

762   nanoparticles and ions on spermatozoa motility of sea trout (Salmo trutta m.

763   Trutta L.). *Aquatic Toxicology*, *211*(August 2018), 11–17.

764   https://doi.org/10.1016/j.aquatox.2019.03.013

765   Kowalski, R. K., & Cejko, B. I. (2019). Sperm quality in fish: Determinants and affecting

766   factors. *Theriogenology*, *135*, 94–108.

767   https://doi.org/10.1016/j.theriogenology.2019.06.009

768   Kurwadkar, S., Pugh, K., Gupta, A., & Ingole, S. (2015). Nanoparticles in the

769   Environment: Occurrence, Distribution, and Risks. *Journal of Hazardous, Toxic,*

770   *and Radioactive Waste*, *19*(3), 04014039. https://doi.org/10.1061/(asce)hz.2153-

771   5515.0000258

772   Labbé, C., & Loir, M. (1991). Plasma membrane of trout spermatozoa: I. Isolation and

773   partial characterization. *Fish Physiology and Biochemistry*, *9*(4), 325–338.

774   https://doi.org/10.1007/BF02265153

775   Labille, J., Slomberg, D., Catalano, R., Robert, S., Apers-Tremelo, M.-L., Boudenne, J.-L.,

776   et al. (2020). Science of the Total Environment. *Science of the Total Environment,*

777   *the*, *706*(C), 136010. http://doi.org/10.1016/j.scitotenv.2019.136010

778   Lan, Z., & Yang, W. X. (2012). Nanoparticles and spermatogenesis: How do

779   nanoparticles affect spermatogenesis and penetrate the blood-testis barrier.

780   *Nanomedicine*, *7*(4), 579–596. https://doi.org/10.2217/nnm.12.20

781   Lankoff, A., Sandberg, W. J., Wegierek-Ciuk, A., Lisowska, H., Refsnes, M., Sartowska,

782   B., Schwarze, P. E., Meczynska-Wielgosz, S., Wojewodzka, M., & Kruszewski, M.

783   (2012). The effect of agglomeration state of silver and titanium dioxide

784   nanoparticles on cellular response of HepG2, A549 and THP-1 cells. *Toxicology*

785   *Letters*, *208*(3), 197–213. https://doi.org/10.1016/j.toxlet.2011.11.006

786   Lodeiro, P., Browning, T. J., Achterberg, E. P., Guillou, A., & El-Shahawi, M. S. (2017).

787   Mechanisms of silver nanoparticle toxicity to the coastal marine diatom

788   *Chaetoceros curvisetus*. *Scientific Reports*, *7*(1), 1–10.

789   https://doi.org/10.1038/s41598-017-11402-x

790   McGillicuddy, E., Murray, I., Kavanagh, S., Morrison, L., Fogarty, A., Cormican, M., et al.

791   (2017). Science of the Total Environment. *Science of the Total Environment, the*,

792   *575*(C), 231–246. http://doi.org/10.1016/j.scitotenv.2016.10.041

793   Magesky, A., & Pelletier, É. (2018). Cytotoxicity and physiological effects of silver

794   nanoparticles on marine invertebrates. *Advances in Experimental Medicine and*

795   *Biology*, *1048*(February), 285–309. https://doi.org/10.1007/978-3-319-72041-

796   8_17

797   Marco-Jiménez, F., Peñaranda, D. S., Pérez, L., Viudes-De-Castro, M. P., Mylonas, C. C.,

798   Jover, M., & Asturiano, J. F. (2008). Morphometric characterization of sharpsnout

799   sea bream (*Diplodus puntazzo*) and gilthead sea bream (*Sparus aurata*)

800   spermatozoa using computer-assisted spermatozoa analysis (ASMA). *Journal of*

801   *Applied Ichthyology*, *24*(4), 382–385. https://doi.org/10.1111/j.1439-

802   0426.2008.01135.x

803   Marques, A., Marçal, R., Pereira, V., Pereira, P., Mieiro, C., Guilherme, S., et al. (2019).

804   Macroalgae-enriched diet protects gilthead seabream (Sparus aurata) against

805   erythrocyte population instability and chromosomal damage induced by aqua-

806   medicines, 1–17. http://doi.org/10.1007/s10811-019-01996-2

807   Mieiro, C. L., Martins, M., Silva, M., Coelho, J. P., Lopes, C. B., Alves, A., Alves, J.,

808   Pereira, E., Pardal, M., Costa, M. H., & Pacheco, M. (2019). Advances on assessing

809   nanotoxicity in marine fish – the pros and cons of combining an *ex vivo* approach

810   and histopathological analysis in gills. *Aquatic Toxicology*, *217*(September),

811   105322. https://doi.org/10.1016/j.aquatox.2019.105322

812 Mohandas, J., Marshall, J., Duggins, G., Horvath, J., & Tiller, D. (1984). Differential

813   distribution of glutathione and glutathione related enzymes in rabbit kidney.

814   Possible implications in analgesic neuropathy. *Cancer Res*, *44*, 5086–5091.

815 Moretti, E., Terzuoli, G., Renieri, T., Iacoponi, F., Castellini, C., Giordano, C., & Collodel,

816   G. (2013). *In vitro* effect of gold and silver nanoparticles on human spermatozoa.

817   *Andrologia*, *45*(6), 392–396. https://doi.org/10.1111/and.12028

818 https://doi.org/10.1016/j.aquaculture.2016.04.021

819 Nielsen, R., Ankamah-Yeboah, I., Llorente, I. (2021) Technical efficiency and

820   environmental impact of seabream and seabass farms, Aquaculture Economics &

821   Management, 25:1, 106-125, DOI: 10.1080/13657305.2020.1840662

822 Ogunsuyi, O. M., Ogunsuyi, O. I., Akanni, O., Alabi, O. A., Alimba, C. G., Adaramoye, O.

823   A., Cambier, S., Eswara, S., Gutleb, A. C., & Bakare, A. A. (2020). Alteration of

824   sperm parameters and reproductive hormones in Swiss mice via oxidative stress

825   after co-exposure to titanium dioxide and zinc oxide nanoparticles. *Andrologia*,

826   *52*(10), 1–17. https://doi.org/10.1111/and.13758

827 Oliveira, H., Spanò, M., Santos, C., & Pereira, M. D. L. (2008). Lead chloride affects

828   sperm motility and acrosome reaction in mice: Lead affects mice sperm motility

829   and acrosome reaction. *Cell Biology and Toxicology*, *25*(4), 341–353.

830   https://doi.org/10.1007/s10565-008-9088-4

831 Olugbodi, J. O., David, O., Oketa, E. N., Lawal, B., Okoli, B. J., & Mtunzi, F. (2020). Silver

832   nanoparticles stimulates spermatogenesis impairments and hematological

833   alterations in testis and epididymis of Male rats. *Molecules*, *25*(5).

834   https://doi.org/10.3390/molecules25051063

835   Özgür, M. E., Balcıoğlu, S., Ulu, A., Özcan, İ., Okumuş, F., Köytepe, S., & Ateş, B.

836   (2018a). The *in vitro* toxicity analysis of titanium dioxide (TiO$_2$) nanoparticles on

837   kinematics and biochemical quality of rainbow trout sperm cells. *Environmental*

838   *Toxicology and Pharmacology*, *62*(June), 11–19.

839   https://doi.org/10.1016/j.etap.2018.06.002

840   Özgür, M. E., Ulu, A., Balcioğlu, S., Özcan, I., Köytepe, S., & Ateş, B. (2018b). The toxicity

841   assessment of iron oxide (Fe$_3$O$_4$) nanoparticles on physical and biochemical

842   quality of rainbow trout spermatozoon. *Toxics*, *6*(4).

843   https://doi.org/10.3390/toxics6040062

844   Özgür, M. E., Ulu, A., Balcioğlu, S., Özcan, I., Okumuş, F., Köytepe, S., & Ateş, B. (2018c).

845   Investigation of Toxicity Properties of Flower-like ZnO Nanoparticles on *Cyprinus*

846   *carpio* Sperm Cells Using Computer-Assisted Sperm Analysis (CASA). *Turkish*

847   *Journal of Fisheries and Aquatic Sciences*, *18*, 771–780.

848   https://doi.org/10.4194/1303-2712-v18

849   Özgür, M. E., Ulu, A., Noma, S. A. A., Özcan, İ., Balcıoğlu, S., Ateş, B., & Köytepe, S.

850   (2020). Melatonin protects sperm cells of *Capoeta trutta* from toxicity of titanium

851   dioxide nanoparticles. *Environ Sci Pollut Res*, *27*, 17843–17853.

852   Özgür, M. E., Ulu, A., Özcan, İ., Balcioglu, S., Ateş, B., & Köytepe, S. (2019).

853   Investigation of toxic effects of amorphous SiO$_2$ nanoparticles on motility and

854   oxidative stress markers in rainbow trout sperm cells. *Environmental Science and*

855   *Pollution Research*, *26*(15), 15641–15652. https://doi.org/10.1007/s11356-019-

856   04941-5

857   Rajeswari, V.D., Eed, E.M., Elfasakhany, A. *et al.* Green synthesis of titanium dioxide

858   nanoparticles using *Laurus nobilis* (bay leaf): antioxidant and antimicrobial

859   activities. *Appl Nanosci* (2021). https://doi.org/10.1007/s13204-021-02065-2

860   Salatin, S., Maleki Dizaj, S., & Yari Khosroushahi, A. (2015). Effect of the surface

861   modification, size, and shape on cellular uptake of nanoparticles. *Cell Biology*

862   *International*, *39*(8), 881–890. https://doi.org/10.1002/cbin.10459

863   Santonastaso, M., Mottola, F., Colacurci, N., Iovine, C., Pacifico, S., Cammarota, M.,

864   Cesaroni, F., & Rocco, L. (2019). *In vitro* genotoxic effects of titanium dioxide

865   nanoparticles (n-TiO2) in human sperm cells. *Molecular Reproduction and*

866   *Development*, *86*(10), 1369–1377. https://doi.org/10.1002/mrd.23134

867   Santonastaso, M., Mottola, F., Iovine, C., Cesaroni, F., Colacurci, N., & Rocco, L. (2020).

868   *In vitro* effects of titanium dioxide nanoparticles (TiO_2NPs) on cadmium chloride

869   ($CdCl_2$) genotoxicity in human sperm cells. *Nanomaterials*, *10*(6), 1–16.

870   https://doi.org/10.3390/nano10061118

871   Shaalan, M., Saleh, M., El-Mahdy, M., & El-Matbouli, M. (2016). Recent progress in

872   applications of nanoparticles in fish medicine: A review. *Nanomedicine:*

873   *Nanotechnology, Biology, and Medicine*, *12*(3), 701–710.

874   https://doi.org/10.1016/j.nano.2015.11.005

875   Shamsi, M. B., Imam, S. N., & Dada, R. (2011). Sperm DNA integrity assays: Diagnostic

876   and prognostic challenges and implications in management of infertility. *Journal*

877   *of Assisted Reproduction and Genetics*, *28*(11), 1073–1085.

878   https://doi.org/10.1007/s10815-011-9631-8

879   Shehata, A. M., Salem, F. M. S., El-Saied, E. M., Abd El-Rahman, S. S., Mahmoud, M. Y.,

880   & Noshy, P. A. (2021). Zinc nanoparticles ameliorate the reproductive toxicity

881   induced by silver nanoparticles in male rats. *International Journal of*

882   *Nanomedicine*, *16*, 2555–2568. https://doi.org/10.2147/IJN.S307189

883   Słowińska, M., Nynca, J., Cejko, B. I., Dietrich, M. A., Horváth, Á., Urbányi, B., Kotrik, L.,

884   & Ciereszko, A. (2013). Total antioxidant capacity of fish seminal plasma.

885   *Aquaculture*, *400–401*, 101–104.

886   https://doi.org/10.1016/j.aquaculture.2013.03.010

887   Taylor, U., Barchanski, A., Petersen, S., Kues, W. A., Baulain, U., Gamrad, L., Sajti, L.,

888   Barcikowski, S., & Rath, D. (2014). Gold nanoparticles interfere with sperm

889   functionality by membrane adsorption without penetration. *Nanotoxicology*,

890   *8*(SUPPL. 1), 118–127. https://doi.org/10.3109/17435390.2013.859321

891   Taylor, U., Tiedemann, D., Rehbock, C., Kues, W. A., Barcikowski, S., & Rath, D. (2015).

892   Influence of gold, silver and gold-silver alloy nanoparticles on germ cell function

893   and embryo development. *Beilstein Journal of Nanotechnology*, *6*(1), 651–664.

894   https://doi.org/10.3762/bjnano.6.66

895   Van Look, K. J. W., & Kime, D. E. (2003). Automated sperm morphology analysis in

896   fishes: The effect of mercury on goldfish sperm. *Journal of Fish Biology*, *63*(4),

897   1020–1033. https://doi.org/10.1046/j.1095-8649.2003.00226.x

898   Vignardi, C. P., Hasue, F. M., Sartório, P. V., Cardoso, C. M., Machado, A. S. D., Passos,

899   M. J. A. C. R., Santos, T. C. A., Nucci, J. M., Hewer, T. L. R., Watanabe, I. S., Gomes,

900   V., & Phan, N. V. (2015). Genotoxity, potential cytotoxicity and cell uptake of

901   titanium dioxide nanoparticles in the marine fish *Trachinotus carolinus* (Linnaeus,

902   1766). *Aquatic Toxicology*, *158*(November), 218–229.

903   https://doi.org/10.1016/j.aquatox.2014.11.008

904   Wang, E., Huang, Y., Du, Q., & Sun, Y. (2017). Silver nanoparticle induced toxicity to

905   human sperm by increasing ROS (reactive oxygen species) production and DNA

906   damage. *Environmental Toxicology and Pharmacology*, *52*(November 2016), 193–

907   199. https://doi.org/10.1016/j.etap.2017.04.010

908   Wassall, S. R., & Stillwell, W. (2009). Biochimica et Biophysica Acta Polyunsaturated

909   fatty acid – cholesterol interactions: Domain formation in membranes. *BBA -*

910   *Biomembranes*, *1788*(1), 24–32. https://doi.org/10.1016/j.bbamem.2008.10.011

911   Xu, M., Li, X. X., Chen, Y., Pitzer, A. L., Zhang, Y., & Li, P. L. (2014). Enhancement of

912   dynein-mediated autophagosome trafficking and autophagy maturation by ROS in

913   mouse coronary arterial myocytes. *Journal of Cellular and Molecular Medicine*,

914   *18*(11), 2165–2175. https://doi.org/10.1111/jcmm.12326

915   Zhang, C., Hu, Z., & Deng, B. (2016). Silver nanoparticles in aquatic environments:

916   Physiochemical behavior and antimicrobial mechanisms. *Water Research*, *88*,

917   403–427. https://doi.org/10.1016/j.watres.2015.10.025
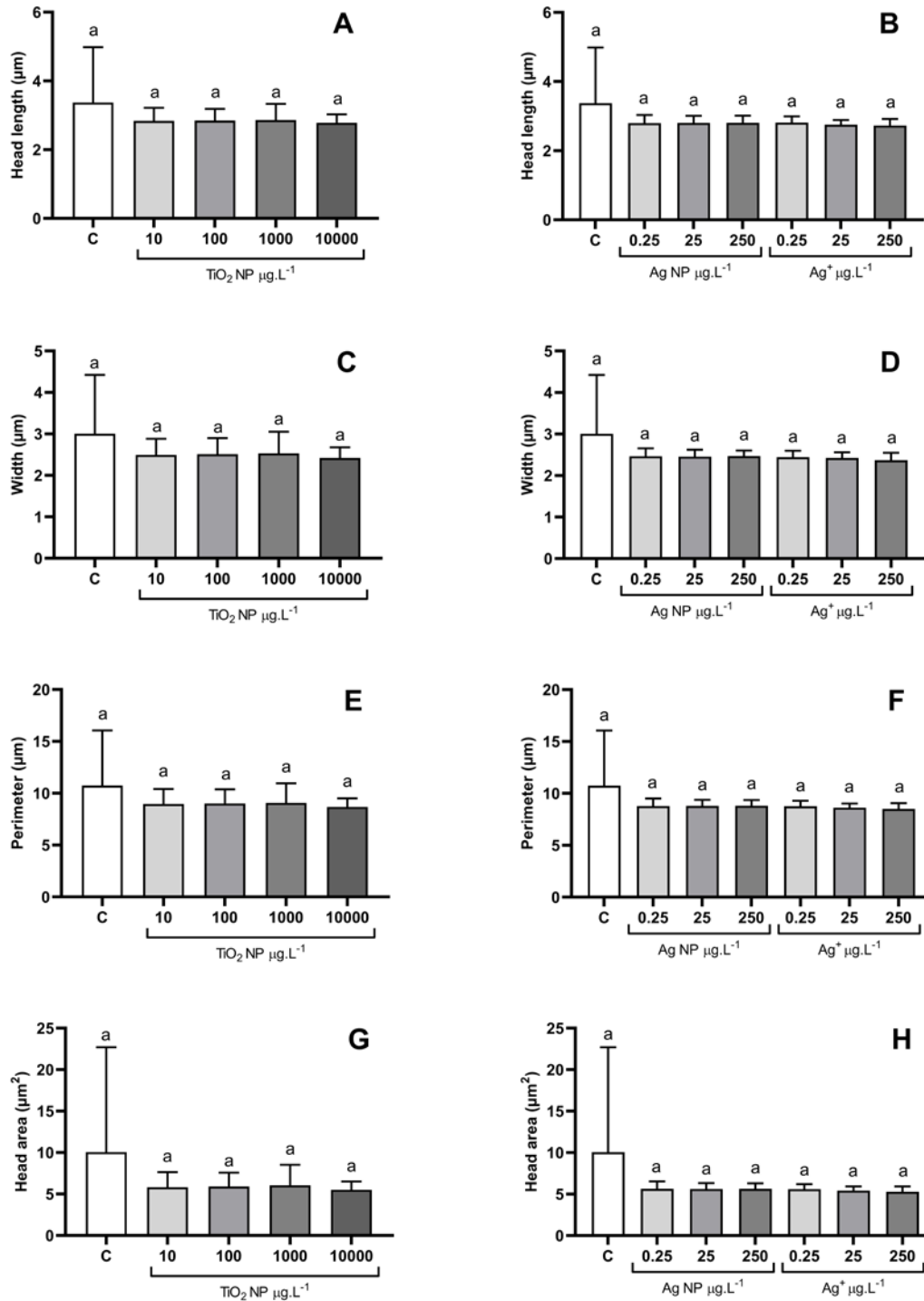
918
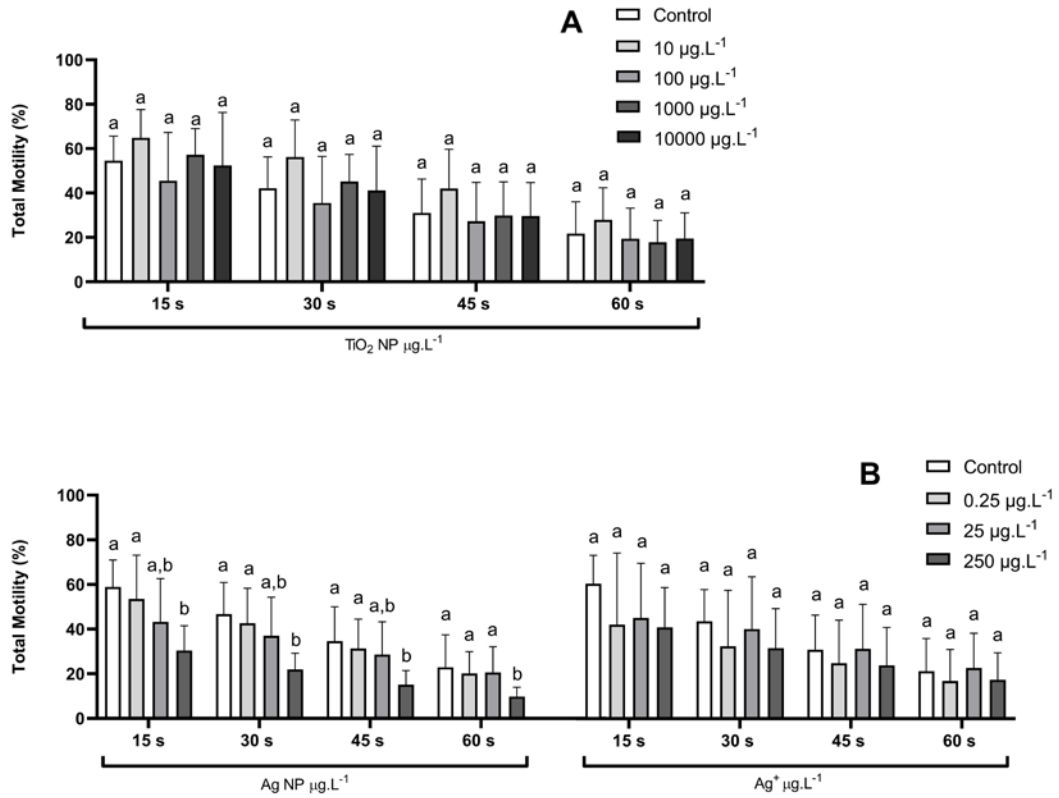
922   Figure 1 - Total motility (%) in spermatozoa of *S. aurata* exposed for 1 h to (A) titanium dioxide
923   nanoparticles (TiO$_2$ NP: 10, 100, 1000 and 10000 µg.L^{-1}), as well as (B) silver nanoparticles (Ag
924   NP: 0.25, 25 and 250 µg.L^{-1}) and silver as AgNO$_3$ ([Ag$^+$]: 0.25, 25 and 250 µg.L^{-1}). Total motility
925   was recorded 15, 30, 45, and 60 sec post-activation. Different lower-case letters denote
926   significant differences (p < 0.05). Columns correspond to mean values and error bars represent
927   the standard deviation.

929
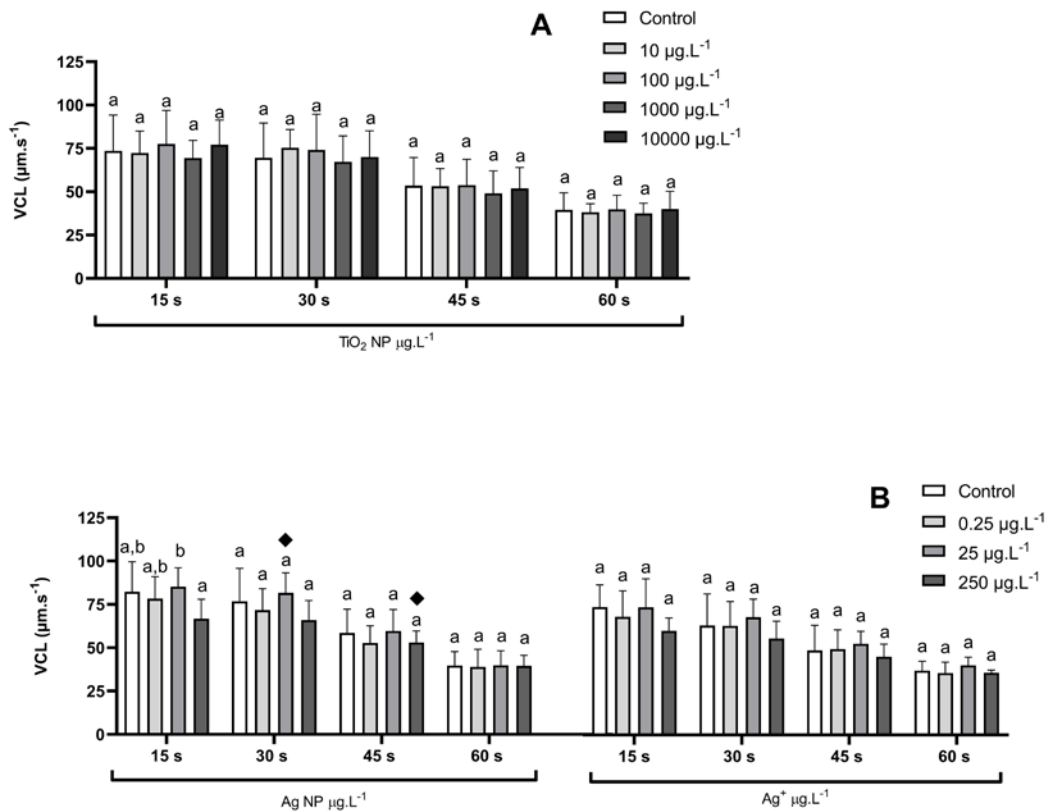
Figure 2 - Curvilinear velocity (VCL) (μm.s^{-1}) in spermatozoa of *S. aurata* exposed for 1 h to (A) titanium dioxide nanoparticles (TiO$_2$ NP: 10, 100, 1000 and 10000 μg.L^{-1}), as well as (B) silver nanoparticles (Ag NP: 0.25, 25 and 250 μg.L^{-1}) and silver as AgNO$_3$ ([Ag$^+$]: 0.25, 25 and 250 μg.L^{-1}). VCL was recorded 15, 30, 45, and 60 sec post-activation. Different lower-case letters denote significant differences among treatments ($p < 0.05$). Significant differences between the corresponding concentrations of Ag NP and Ag$^+$ is depicted by ($\blacklozenge$) ($p < 0.05$). Columns correspond to mean values and error bars represent the standard deviation.
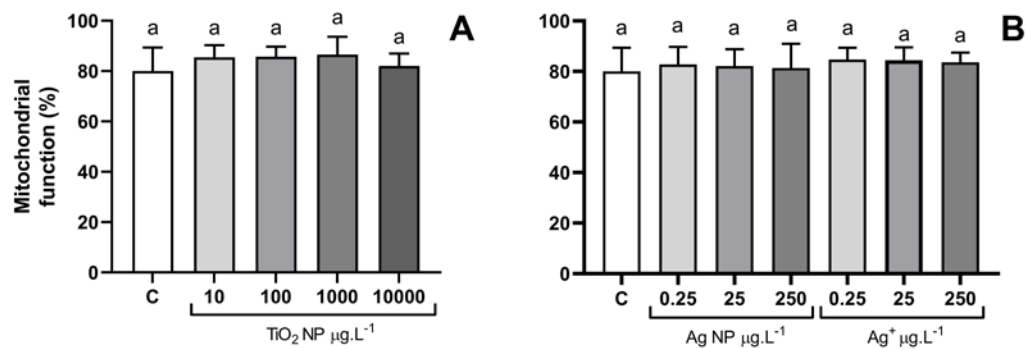
937

Figure 3 - Morphometric parameters (μm^2) in spermatozoa of *S. aurata* exposed for 1 h to titanium dioxide nanoparticles (TiO_2 NP: 10, 100, 1000 and 10000 $\mu g.L^{-1}$), as well as silver nanoparticles (Ag NP: 0.25, 25 and 250 $\mu g.L^{-1}$) and silver as $AgNO_3$ ([Ag^+]: 0.25, 25 and 250 $\mu g.L^{-1}$). Different lower-case letters denote significant differences ($p < 0.05$). Columns correspond to mean values and error bars represent the standard deviation. C - control.

943
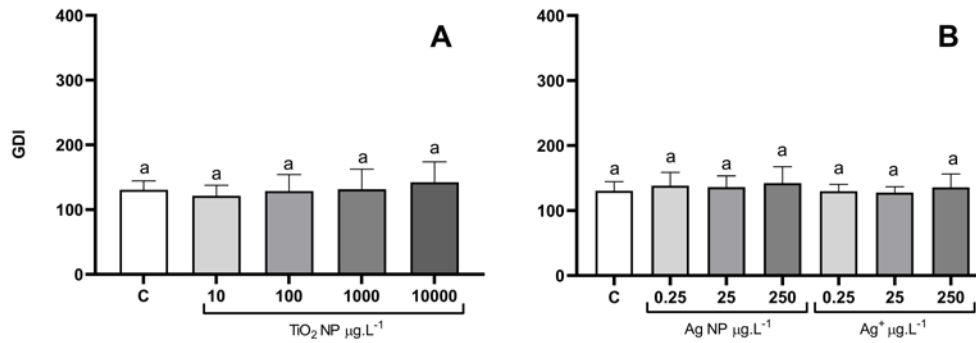
Figure 4 - Genetic damage indicator (GDI; expressed in arbitrary units) in spermatozoa of *S. aurata* exposed for 1 h to (A) titanium dioxide nanoparticles (TiO$_2$ NP: 10, 100, 1000 and 10000 µg.L^{-1}), as well as (B) silver nanoparticles (Ag NP: 0.25, 25 and 250 µg.L^{-1}) and silver as AgNO$_3$ ([Ag$^+$]: 0.25, 25 and 250 µg.L^{-1}). Different lower-case letters denote significant differences (p < 0.05) in relation to control. Columns correspond to mean values and error bars represent the standard deviation. C - control.
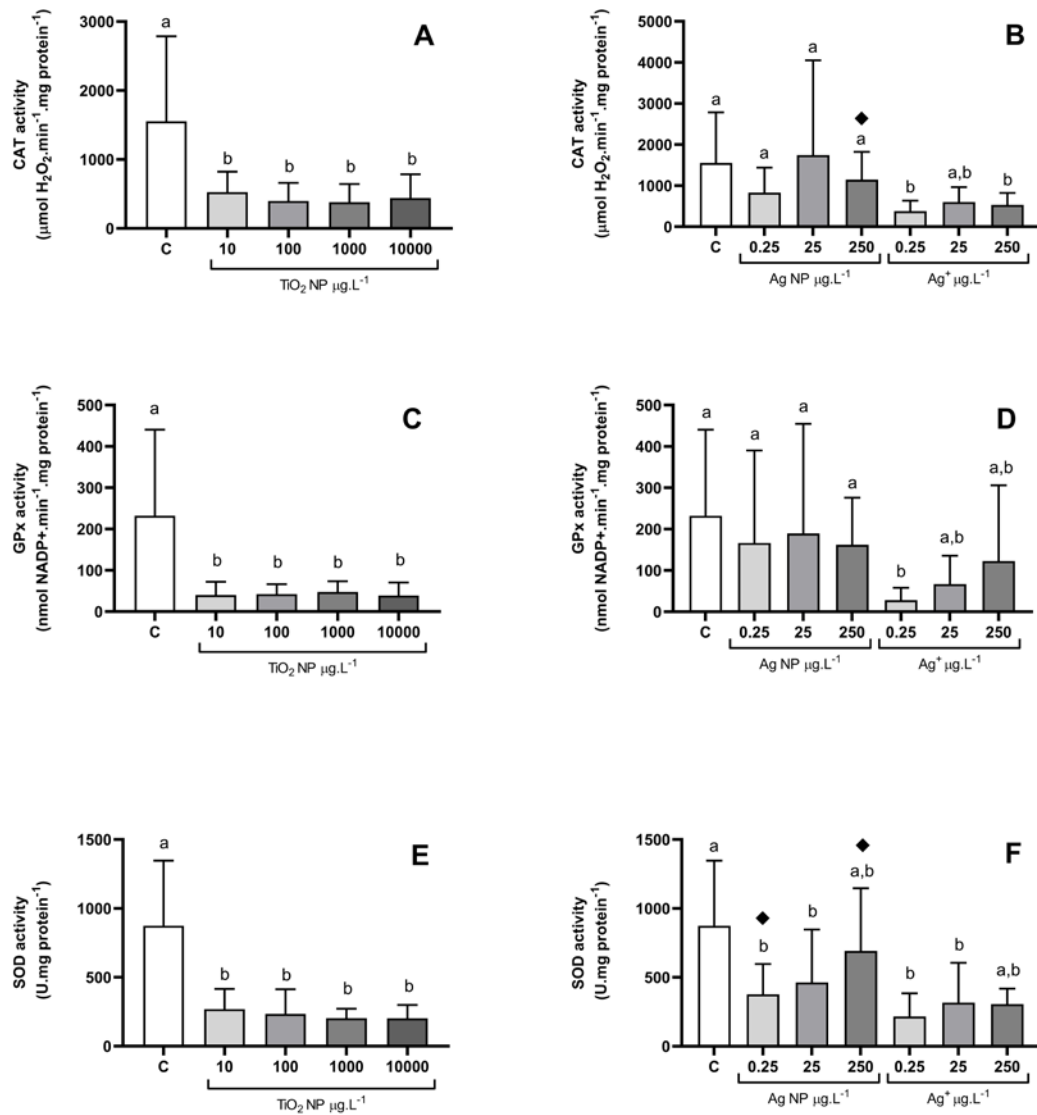
950

951

Figure 5 - Mitochondrial function (PI+Rh123+/PI-Rh123+) in spermatozoa of *S. aurata* exposed for 1 h to (A) titanium dioxide nanoparticles (TiO$_2$ NP: 10, 100, 1000 and 10000 µg.L^{-1}), as well as (B) silver nanoparticles (Ag NP: 0.25, 25 and 250 µg.L^{-1}) and silver as AgNO$_3$ ([Ag$^+$]: 0.25, 25 and 250 µg.L^{-1}). Different lower-case letters denote significant differences (p < 0.05). Columns correspond to mean values and error bars represent the standard deviation. C - control.

957

Figure 6 - Antioxidant responses in spermatozoa of *S. aurata* exposed for 1 h to (A) titanium dioxide nanoparticles (TiO$_2$ NP: 10, 100, 1000 and 10000 µg.L^{-1}), as well as (B) silver nanoparticles (Ag NP: 0.25, 25 and 250 µg.L^{-1}) and silver as AgNO$_3$ ([Ag$^+$]: 0.25, 25 and 250 µg.L^{-1}). Different lower-case letters denote significant differences (p < 0.05) in relation to control. Significant differences between the corresponding concentrations of Ag NP and Ag$^+$ is depicted by (◆) (p < 0.05). Columns correspond to mean values and error bars represent the standard deviation.